Scripta Materialia 179 (2020) 45–48

Contents lists available at ScienceDirect

Scripta Materialia

journal homepage: www.elsevier.com/locate/scriptamat

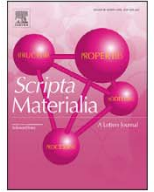

Extremely rapid grain growth in scallop-type Cu_6Sn_5 during solid–liquid interdiffusion reactions in micro-bump solder joints

A.M. Gusak[a], K.N. Tu[b,c], Chih Chen[c,*]

[a] Department of Physics, Cherkasy National University, Ukraine
[b] Department of Materials Science and Engineering, University of California at Los Angeles, Los Angeles, CA, USA
[c] Department of Materials Science and Engineering, National Chiao Tung University, Hsinchu, Taiwan, ROC

ARTICLE INFO

Article history:
Received 23 November 2018
Revised 2 December 2019
Accepted 4 January 2020

Keywords:
Scallop of Cu_6Sn_5
Grain growth
Micro-bump
Solder joint technology
Liquid channel

ABSTRACT

In 3D IC technology, when the size of the micro-bump solder joint is reduced to 10 µm, the scallop-type Cu_6Sn_5 grains on opposite sides of the joint can interact directly by contacting each other during the solid–liquid interdiffusion reaction. Upon contact, an extremely rapid grain growth of the scallops occurs. We propose that the liquid solder wets the grain boundary between scallops and provides an extremely fast kinetic path of liquid channel for grain growth. The width of the liquid channel has been estimated to be about 1.5 nm. This is a unique phenomenon observed in micro-bump solid joints.

© 2020 Acta Materialia Inc. Published by Elsevier Ltd. All rights reserved.

In solid–liquid interdiffusion (SLID) reactions of solder joint formation, the study on growth of intermetallic compounds (IMC) is essential, especially scallop-type Cu_6Sn_5. [1–10] When the solder joint size is large as in C-4 s (controlled-collapsed-chip-connection), which has a diameter of about 100 µm, the scallop-type IMC on both sides of the joint are far apart, so they do not interact directly. The growth kinetics of the scallops were found to be a non-conservative ripening reaction because the total volume of scallops increases with time, yet the total surface area of scallops is constant, thus it obeys the constraint of a constant surface area or a constant contact area. The volume increase comes from the rapid diffusion of Cu via the channels between scallops, and the channels are assumed to be liquid channels. [3] The scallop-type ripening is different from the classic ripening model according to LSW theory, [5,6] which assumes a constant volume during ripening.

In micro-bumps for 3D IC, the thickness of the solder is only 10 µm, [11–15] so the two rows of scallops, on the upper and lower interfaces, can actually contact each other as shown in Fig. 1. What has been a very surprising discovery is that when the two opposing scallops contacts, they appear to merge quickly into a single columnar grain without forming a grain boundary between them [11]. There have been several reports on this unique finding [7–10], yet no clear model was presented to explain the mechanism. Here, we propose the existence of a liquid channel between the two scallops under direct contact, and the fast diffusion along and across the liquid channel leading to the extremely rapid grain growth. Our calculation supports the experimental finding. The width of the liquid channel is estimated to be about 1.5 nm. Up to now, it is still very difficult to experimentally measure the liquid channel width because it solidifies during sample preparation for SEM and TEM observations.

Fig. 1(a) and (b), respectively, shows scanning electron microscopy (SEM) and EBSD cross-sectional images of a SnAg solder of about 10 µm in thickness between two Cu microbumps reflowed at 260 °C for 3 mins. There are two rows of Cu_6Sn_5 scallops (the upper and the lower) facing each other in these figures. The solder is almost completely consumed by IMC formation, as indicated by one of the arrows in the figure. With one more minute of reflow at 260 °C, most of the Cu_6Sn_5 scallops have grown across the entire joint, as illustrated in Fig. 1(c). The results indicate that the grain growth of scallop-type Cu_6Sn_5 in molten solder is very fast.

It is known that the grain boundaries between grains of Cu_6Sn_5 can be wetted by liquid solder [3,16]. Experimentally, a sample of the scallop-type IMC was annealed below the melting point of the solder at 150 °C for 24 h, the scallops disappeared and transformed to a layer-type IMC with the formation of grain boundaries between the IMC grains. When the excess solder was etched away, the SEM image of the top IMC surface reveals a polycrystalline microstructure, as shown in Fig. 2(a). The cross-sectional image showed that the grain boundaries are vertical lines [16]. However,

* Corresponding author.
E-mail address: chih@mail.nctu.edu.tw (C. Chen).

https://doi.org/10.1016/j.scriptamat.2020.01.005
1359-6462/© 2020 Acta Materialia Inc. Published by Elsevier Ltd. All rights reserved.

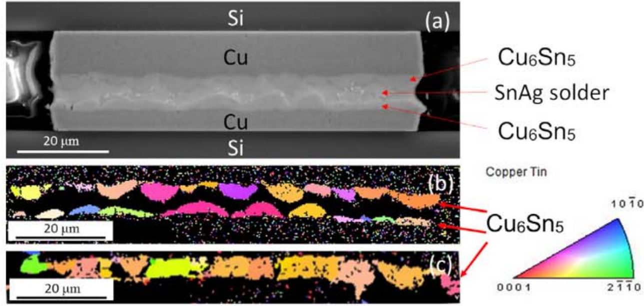

Fig. 1. (a) SEM image showing a microbump with Cu under-bump metallization on both sides after reflow at 260 °C for 3 min. (b) EBSD orientation image maps in the rolling direction for the Cu_6Sn_5 intermetallic compounds. (c) Another microbump reflowed for 4 min at 260 °C.

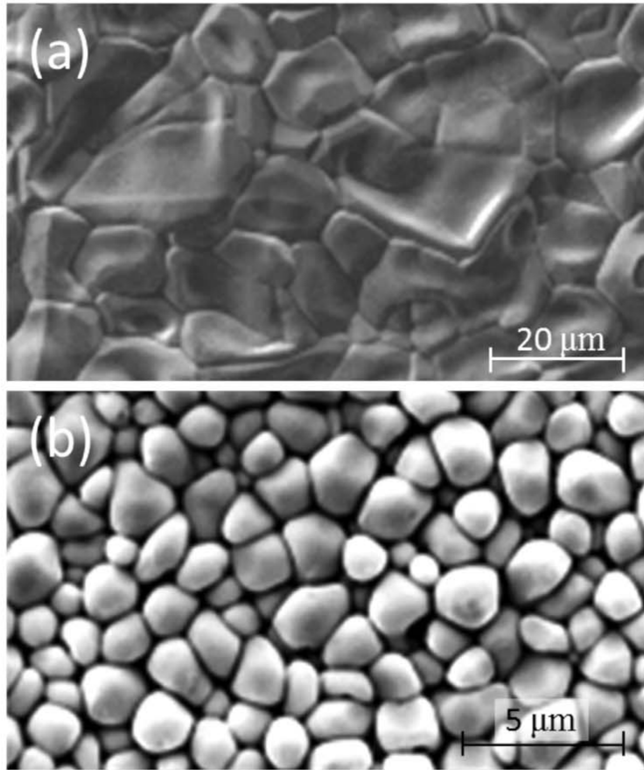

Fig. 2. (a) The top-view SEM image of surface of Cu_6Sn_5 polycrystalline grains after solid state aging at 150 °C for 24 h and followed by the etching of the unreacted solder away. (b) The top-view SEM image of the surface of scallop-type Cu6Sn_5 grains right after SLID and followed by etching of the unreacted solder away.

when a layer of solder was re-deposited on the top surface of the layer-type IMC and annealed above the melting point of the solder for just 1 min, the molten solder wetted the IMC grain boundaries. This is verified by cooling the sample to room temperature and etching the excess solder away, and the top surface is shown in Fig. 2(b), where the scallop-type IMC reappeared with deep valleys or channels between them, but no grain boundaries.

The condition of full wetting is given below

$$\gamma_{GB} \equiv \gamma_{\eta/\eta} > 2\gamma_{\eta/liq} \tag{1}$$

where $\gamma_{GB} = \gamma_{\eta/\eta}$, $\gamma_{\eta/liq}$ are surface energy of grain boundary of Cu_6Sn_5, and interfacial energy between Cu_6Sn_5 and liquid solder, respectively. In general, grain boundary energy between adjacent grains depends on the mis-orientation between them. The highest grain boundary energy is realized at the high-angle grain boundaries, and such boundaries are certain to be wetted. If the boundary is a low-angle type, such as a low angle tilt-type or twist-type, it has a low grain boundary energy, so that the wetting condition of Eq. (1) may not be valid.

Therefore, we may distinguish two cases:

(A) Immediate merging with the formation of a small angle grain boundary

If for the opposite IMC grains, $\gamma_{GB} \equiv \gamma_{\eta/\eta} < 2\gamma_{\eta/liq}$, upon meeting they will just merge into one column, forming a solid small angle grain boundary between them. To observe this grain boundary directly at a cross-sectional image could be a problem because of small mis-orientation and close image contrast.

(B) Consuming one grain by the opposite growing grain due to atomic flux crossing a narrow liquid channel between them

Let Eq. (1) of the two opposite grains to be valid. When these two grains approach one another to the distance, δ, which is the width of liquid channel, the direct diffusion from one grain to the other across the liquid channel becomes the main reason of the growth of one grain at the expense of the other grain. The thickness of the liquid channel is of nanoscale, to be proven both experimentally and theoretically later, which makes the gradient of chemical potentials between neighboring grains larger, even in the case when the difference of Gibbs-Thomson potentials $\gamma_{\eta/melt}\Omega/R$ between them is not that large [17,18]:

$$|grad\mu| = \frac{|\mu_2 - \mu_1|}{\delta} = \frac{\left|\gamma_{\eta/melt}\Omega/R_2 - \gamma_{\eta/melt}\Omega/R_1\right|}{\delta} = \frac{\gamma_{\eta/melt}\Omega}{\delta}\left|\frac{1}{R_2} - \frac{1}{R_1}\right| \tag{2}$$

Here Ω is the atomic volume, the curvature radius is positive for a convex shape and negative for a concave shape.

An initial configuration with both convex shapes at the moment of contact between opposite scallops is shown in Fig. 3a. We may expect a transition period when the remnants of bulk liquid solder between the scallops disappear due to the continuing fluxes of Cu both from the “bottom” and “ceiling” via the liquid channels. As a result, we expect the formation of normal “grain” structure but with a significant part of large angle “grain boundary” being wetted by liquid solder, thus, actually becoming the liquid interlayers of critical thickness, δ, as shown in Fig. 3b. In an extreme case of Fig. 3c, when two opposite grains are connected by a liquid interlayer of constant curvature of 1/R, the two radii are almost equal by absolute value and opposite by sign, so that $|\frac{1}{R_2} - \frac{1}{R_1}| = \frac{2}{R}$.

We shall evaluate this with the simplest situation in Fig. 3c. The Cu flux density over the channel is [19]:

$$J_{Cu} = \frac{1}{\Omega}\frac{C_{Cu}^{melt}D_{Cu}^{melt}}{kT}\frac{\mu_2 - \mu_1}{\delta}\left(\frac{atoms}{m^2 s}\right) \tag{3}$$

Here C_{Cu}^{melt} is an atomic fraction of melted Cu and C_{Cu}^{melt}/Ω is the number of Cu atoms per unit volume of the liquid. Obviously, the Sn flux is accommodated to the Cu flux in order to form Cu_6Sn_5, because we have plenty of Sn atoms in the remaining liquid solder phase. The local velocity of interface movement is determined by the flux balance equation below,

$$V = \frac{1}{C_i - C_{Cu}^{melt}}(\Omega J_{Cu} - 0) = \frac{C_{Cu}^{melt}D_{Cu}^{melt}}{\left(C_i - C_{Cu}^{melt}\right)kT}\frac{\mu_2 - \mu_1}{\delta}\left(\frac{atoms}{m^2 s}\right) \tag{4}$$

Here $C_i \equiv C_{Cu}^{\eta}$ is the atomic fraction of Cu in Cu_6Sn_5, and “0” is the flux inside grain. Using Eq. (2) for driving force, we obtain

$$V \approx \frac{4C_{Cu}^{melt}D_{Cu}^{melt}}{\left(C_i - C_{Cu}^{melt}\right)kT}\frac{\gamma_{\eta/melt}\Omega}{R\delta}. \tag{5}$$

We take the following reasonable parameters:

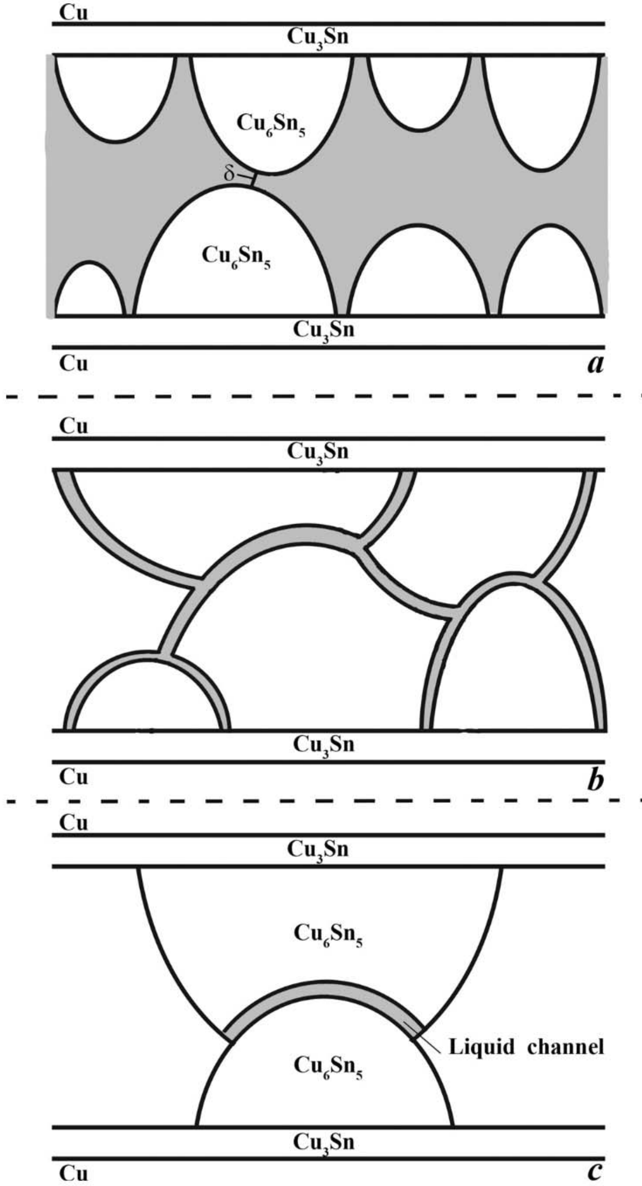

Fig. 3. Schematic diagram of the meeting of two Cu_6Sn_5 scallop-type grains with a liquid channel between them: (a) Initial touching of opposite scallops, (b) Formation of grain structure with fully wetted grain boundaries and (c) Marginal case of fastest grain growth by direct consuming of some grain by the opposite one.

$C_{Cu}^{\eta} = \frac{6}{11}$, $C_{Cu}^{melt} = 0.02$, $\gamma = 0.5\frac{J}{m^2}$, $\Omega = 1.8 \cdot 10^{-29}\frac{m^3}{atom}$, $D_{Cu}^{melt} = 10^{-9}\frac{m^2}{s}$, $R = 5 \cdot 10^{-6}$m, $\delta = 1.5 \cdot 10^{-9}$m (Here $C_{Cu}^{\eta} = \frac{6}{11}$ is a stoichiometric fraction of Cu in η-phase, $C_{Cu}^{melt} = 0.02$is an equilibrium atomic fraction of copper in molten solder in equilibrium with η-phase, estimated from CALPHAD data [20–22]. Surface tension between solid Cu_6Sn_5 and liquid solder is estimated according to Amore et al. [23]. Atomic volume Ω can be taken, for example, from [24]. Diffusivity of copper in tin and corresponding interdiffusivity in Sn–Cu liquid alloy was estimated, for example, in [25,26]. Channel width has several estimations of the same order of magnitude: in [27] by indirect methods it was estimated as 2.5 nm. In [26] it was estimated as 0.7–0.8 nm. So, with our rough estimations we assume it to be somewhere in between such as 1.5 nm.) Then we obtain $V = 1.35 \cdot 10^{-5}\ \frac{m}{s}$. Thus, the time to form a columnar grain of H = 30 μm from two contacting scallops should be about $(30 \times 10^{-6}/2)/(13.5 \times 10^{-6}) = 1$ s. Thus, when the two IMC grains contacts each other, they can merge into one right away.

Now we consider a more general situation, corresponding to Fig. 3b. We may expect the normal grain growth but with mobility determined by fast diffusion across liquid interlayers. For a rough evaluation, we will use the well-known mean-field Hillert model [28] of normal grain growth in 3D-polycrystalline, in which the growth/shrinkage rate of any grain size is determined by the equation

$$\frac{dR}{dt} = \frac{C_{Cu}^{melt} D_{Cu}^{melt}}{\left(C_{Cu}^{Cu_6Sn_5} - C_{Cu}^{melt}\right)kT} \frac{\mu^{mean-field} - \mu(R)}{\delta} = \frac{C_{Cu}^{melt} D_{Cu}^{melt}}{\left(C_{Cu}^{Cu_6Sn_5} - C_{Cu}^{melt}\right)kT} \frac{2\gamma\Omega}{\delta}\left(\frac{1}{R_{cr}} - \frac{1}{R}\right) \quad (6)$$

Using the Hillert parabolic solution for 3D case of normal grain growth, we may evaluate the change of the squared mean radius as

$$\Delta\bar{R}^2 \approx 0.2 \frac{C_{Cu}^{melt} D_{Cu}^{melt}}{\left(C_{Cu}^{Cu_6Sn_5} - C_{Cu}^{melt}\right)kT} \frac{2\gamma\Omega}{\delta} t\ . \quad (7)$$

Result (7) allows us to estimate the time of grain growth from the contact between opposing scallops (when, roughly, $R = H/2$) to single grain size from "bottom" to "top" (roughly, $R = H$).

Taking roughly $\Delta\bar{R}^2 \approx H^2 - (H/2)^2 = \frac{3}{4}H^2$, $H \approx 3 \cdot 10^{-5}$m, we obtain,

$$t \approx \frac{0.75H^2\left(C_{Cu}^{Cu_6Sn_5} - C_{Cu}^{melt}\right)kT\delta}{2\gamma\Omega C_{Cu}^{melt} D_{Cu}^{melt}} \approx 20\text{s}$$

The time is longer than that in case (c), but still much faster than the normal scallop growth in solid state reaction.

We compare this result with the time needed to grow a scallop of 15 μm size in the usual flux-driven ripening process [3]:

$$R^3 \approx \frac{9}{2} \frac{D_{Cu}^{melt}\left(C_{Cu}^{melt/\eta} - C_{Cu}^{melt/\varepsilon}\right)}{C_{Cu}^{\eta}} \delta \cdot t, \quad (8)$$

here $C_{Cu}^{melt/\eta}, C_{Cu}^{melt/\varepsilon}$ are the atomic fractions of melted Cu for equilibrium state, respectively, with phases $\eta(Cu_6Sn_5)$and $\varepsilon(Cu_3Sn)$, their difference is a little bit less than one percent [26]. Thus,

$$t \approx \frac{2C_{Cu}^{\eta}R^3}{9D_{Cu}^{melt}\left(C_{Cu}^{melt/\eta} - C_{Cu}^{melt/\varepsilon}\right)\delta} \approx \frac{12/11 * 10^{-15}}{9 \cdot 10^{-9}10^{-2}2 \cdot 10^{-9}} \approx 6000\text{s}$$

The difference between 1 s, 20 s, and 6000 s is pronounced, and the reason is that the usual flux driven ripening growth is controlled by the in-flux of Cu in the ripening zone via the narrow liquid channels. In contrary, at the final stage of grain growth between the opposing Cu_6Sn_5, the flux goes only from grain to grain across the channel, which has a very narrow width δ of one-two nanometers.

About theoretical estimation of the liquid channel width, we note that during last decade several attempts were made, both experimentally and theoretically [26,27,29,30]. So far, it is difficult to observe it directly because the channel will freeze and transform into a grain boundary in sample preparation. Strictly speaking, we have a paradox: due to Gibbs free energy profit of reaction, the liquid Sn tends to react with coming Cu atoms, transforming the channels into IMC structure. On the other hand, this transformation should lead to emerging of a large-angle grain boundary, instead of two IMC/melted interfaces, which is non-profitable according to Eq. (1).

Consider a channel with a width of δ between two neighboring grains. Due to supersaturation of melted Cu in flux-driven ripening [3], some heterogeneous fluctuation creates the nucleus of Cu_6Sn_5 phase which represents a kind of solid bridge between the two grains. Let's suppose this bridge has the shape of cylinder (disk)

/

with a height δ and radius R. The change of Gibbs free energy due to formation of a disk is equal to

$$\Delta G(R,\delta) = \left(-\frac{\Delta g_{melt\to\eta}}{\Omega}\right)\pi R^2\delta + \left(\gamma_{\eta/\eta} - 2\gamma_{\eta/liq}\right)\cdot\pi R^2 + \gamma_{\eta/liq}\cdot 2\pi R\delta \quad (9)$$

The first term is proportional to the bulk energy of transformation per atom, $\Delta g_{melt\to\eta}$. As analyzed in [3] and later in more details in [19], it can be reduced by the driving force $\Delta g_{\varepsilon+solder\to\eta}$ of the reaction $2Cu_3Sn+3Sn->Cu_6Sn_5$ (Cu atoms come to the melt from the layer of Cu_3Sn phase via the liquid channels). The second term corresponds to change from two solid/liquid interfaces into one grain-boundary. The third term corresponds to the cylinder side surface. After rearrangement, we end up with:

$$\Delta G(R,\delta) = \left(\gamma_{\eta/\eta} - 2\gamma_{\eta/liquid} - \frac{\Delta g_{\varepsilon+solder\to\eta}}{\Omega}\delta\right)\cdot\pi R^2 + \gamma_{\eta/liq}\cdot 2\pi R\delta \quad (10)$$

The dependence of Gibbs free energy of cylinder radius R varies at different fixed widths of δ - larger or smaller than some "critical" width,

$$\delta^* = \frac{\gamma_{\eta/\eta} - 2\gamma_{\eta/liquid}}{\Delta g_{\varepsilon+solder\to\eta}}\Omega. \quad (11)$$

under which further filling of the liquid channel by the Cu_3Sn phase is impossible. Namely, dependence of Eq. (10) on $\Delta G(R)$

(1) has a nucleation type form with barrier (saddle-point) at $\delta > \delta^*$,
(2) monotonically increases with increasing R at $\delta < \delta^*$.

To numerically estimate Eq. (11), we take $\Delta g_{\varepsilon+solder\to\eta} \approx 0.4\frac{J}{atom}$, $\Omega \approx 1.8\cdot 10^{-29}m^3$ [29,24]. To evaluate the difference $\gamma_{\eta/\eta} - 2\gamma_{\eta/liquid}$ is a complicated problem. In case of full wetting it is positive (condition of liquid channel formation), but the exact value depends on misorientation of neighboring scallops and should be calculated, for example, by DFT. For sure, this value should be between 0 and $1\,J/m^2$ [23] corresponding (according to Eq. [11]) to the range $0 < \delta^* < 4.5\,nm$. To obtain $\delta^* = 1.5\,nm$ (value used in the above estimate of the rapid grain growth), $\gamma_{\eta/\eta} - 2\gamma_{\eta/liquid}$ should be about $0.33\,J/m^2$.

In summary, when the size of micro-bump solder joint is reduced to 10 μm in 3D IC technology, the scallop-type grains of Cu_6Sn_5 on the opposite sides of the joint can interact directly by contacting each other to form a grain boundary during the SLID reaction. Upon touching, an extremely rapid grain growth of the scallop-type grains occurs if the grain boundary is large angle and has high energy. We propose that this is because the liquid solder wets the large angle grain boundary and the wetting channel provide an extremely fast kinetic path for grain growth. On the other hand, if the grain boundary is a small angle of tilt-type or twist-type, the liquid solder will not be able to wet it, so no rapid grain growth occurs. Furthermore, in large size C-4 solder joints, the opposite IMC grains will not contact each other, so no rapid grain growth was observed. The rapid grain growth of Cu_6Sn_5 is a unique phenomenon in micro-bump solid joint technology.

Declaration of Competing Interest

None.

Acknowledgment

The authors acknowledge the financial support from the Ministry of Science and Technology, Taiwan, under Grants MOST-108-3017-F-009-003, MOST-108-3017-F-009-004; and Research of Excellence (RoE) Program, MOST 108-2633-E-009-001. Also, in part this work was supported by Ministry of Education and Science of Ukraine. One of the authors (AG) is grateful to Dept. MSE in NCTU for hospitality.

References

[1] H. Kim, K.N. Tu, Appl. Phys. Lett. 67 (14) (1995) 2002–2004.
[2] H. Kim, K.N. Tu, Phys. Rev. B 53 (23) (1996) 16027.
[3] A. Gusak, K.N. Tu, Phys. Rev. B 66 (11) (2002) 115403.
[4] J.O. Suh, K.N. Tu, N. Tamura, Appl. Phys. Lett. 91 (5) (2007) 051907.
[5] I.M. Lifshitz, V.V. Slyozov, J. Phys. Chem. Solids 19 (1–2) (1961) 35–50.
[6] C. Wagner, Z. Electrochem. 65 (1961) 581–591.
[7] V. Attari, S. Ghosh, T. Duong, R. Arroyave, Acta Mater. 160 (2018) 185–198.
[8] T.L. Yang, J.Y. Wu, C.C. Li, S. Yang, C.R. Kao, J. Alloys Compd. 647 (2015) 681–685.
[9] P. Yao, X. Li, X. Liang, B. Yu, F. Jin, Y. Li, Mater. Charact. 131 (2017) 49–63.
[10] Z.H. Zhang, M.Y. Li, C.Q. Wang, Intermetallics 42 (2013) 52–55.
[11] C. Hang, Y. Tian, R. Zhang, D.S. Yang, J. Mater. Sci.: Mater. Electron. 24 (2013) 3905–3913.
[12] H.Y. Hsiao, C.M. Liu, H.W. Lin, T.C. Liu, C.L. Lu, Y.S. Huang, C. Chen, K.N. Tu, Science 336 (2012) 1007–1010.
[13] Y.A. Shen, C. Chen, Scr. Mater. 128 (2017) 6–9.
[14] C. Chen, D. Yu, K.N. Chen, MRS Bull. 40 (3) (2015) 257–263.
[15] H.W. Lin, J.L. Lu, C.M. Liu, C. Chen, D. Chen, J.C. Kuo, K.N. Tu, Acta Mater. 61 (2013) 4910–4919.
[16] K.N. Tu, F. Ku, T.Y. Lee, J. Electron. Mater. 30 (9) (2001) 1129–1132.
[17] J.W. Gibbs, Trans. Connecticut Acad. Arts Sci. 3 (1878) 343–524.
[18] S.W. Thomson, Philos. Mag. 42 (282) (1871) 448–452.
[19] K.N. Tu, J.W. Mayer, L.C. Feldman, Electronic Thin Film Science for Electrical Engineers and Materials Scientists, Macmillan, New York, 1996.
[20] A. Dinsdale, Calphad 15 (4) (1991) 317–425, doi:10.1016/0364-5916(91)90030-N.
[21] J.H. Shim, C.S. Oh, B.J. Lee, D.N. Lee, Z. Metallkd. 87 (3) (1996) 205–212 https://www.osti.gov/etdeweb/biblio/228997.
[22] F. Hodaj, O. Liashenko, A.M. Gusak, Philos. Mag. Lett. 94 (4) (2014) 217–224, doi:10.1080/09500839.2014.886782.
[23] S. Amore, E. Ricci, T. Lanata, R. Novakovic, J. Alloys Compd. 452 (1) (2008) 161–166, doi:10.1016/j.jallcom.2007.01.178.
[24] J.Y. Song, J. Yu, T.Y. Lee, Scr. Mater. 51 (2) (2004) 167–170, doi:10.1016/j.scriptamat.2004.03.032.
[25] M. Mouas, J.G. Gasser, S. Hellal, B. Grosdidier, A. Makradi, S. Belouettar, EPJ Web Conf. 15 (2011) 01013 EDP Sciences, doi:10.1051/epjconf/20111501013.
[26] O.Y. Liashenko, F. Hodaj, Acta Mater. 99 (2015) 106–118, doi:10.1016/j.actamat.2015.07.066.
[27] J.O. Suh, K.N. Tu, G.V. Lutsenko, A.M. Gusak, Acta Mater. 56 (2008) 1075–1083.
[28] M. Hillert, Acta Metall. 13 (3) (1965) 227–238.
[29] O. Liashenko, A.M. Gusak, F. Hodaj, J. Mater. Sci.: Mater. Electron. 25 (10) (2014) 4664–4672.
[30] A.M. Gusak, O.Y. Liashenko, F. Hodaj, Cherkasy Univ. Bull.: Phys. Math. Sci. 269 (2013) 3–18.

/